Turbulent convection and differential rotation in spherical shells

By V. Olshevsky, Ch. Liang, F. Ham, N. N. Mansour AND A. G. Kosovichev

1. Motivation and objective

Rotation is a general phenomenon in astrophysical systems on scales from planets to giant galaxy clusters. It is established during the formation of the system under gravitational compression. Typically the rotation rate is greatly enhanced during this process (Thompson *et al.* 2003). Rotation of stars defines their shapes and drives the internal circulation which redistributes chemical elements and angular momentum (Maeder 2009). The differential rotation of the Sun is thought to be a key ingredient of its dynamo, a driver of the 11-year activity cycle (Schrijver & Zwaan 2000).

The difference in the speed of sunspots at different latitudes was noticed in Galileo's first observations of sunspots. Since then differential rotation was observed by tracking different photospheric features and by spectral observations of the limb. The angular speed on the visible surface of the Sun smoothly decreases from the equator to the poles. The approximate law, deduced from observations, is usually in the form of

$$\Omega(\Theta) = A - B\cos^2\Theta - C\cos^4\Theta, \tag{1.1}$$

where Ω is angular speed, Θ is co-latitude, and the coefficients A, B, C depend on the observing method (Paternò 2010; Thompson *et al.* 2003).

Global helioseismology enables measurements of solar rotation profiles in deeper layers, the convective zone, and radiative core. According to the present picture, the solar radiative core extends approximately to $0.69R_\odot$, and rotates uniformly. At larger radii, in the convective zone, the rotation profile has complex dependence on radius and latitude. The core and the convective zone are separated by a thin layer called the solar tachocline. The thickness of the tachocline according to different estimates is about $0.03R_\odot$. This layer may play a crucial role in the global dynamo, and resolving it in simulations is an important issue. Turbulent convection, which drives the differential rotation, produces other interesting phenomena such as supergranulation, torsional oscillations, and meridional circulation. These are extensively studied by local helioseismology techniques. Overviews of helioseismological studies of solar internal rotation and associated phenomena were given by, e.g., Christensen-Dalsgaard (2002); Thompson *et al.* (2003); Miesch (2005); Gizon *et al.* (2010).

Studies of stellar rotation and turbulent convection are great challenges for theoreticians. The theory of stability and evolution of rotating stars has established a separate branch of astrophysics (Tassoul 1978; Maeder 2009). Estimated Reynolds numbers in the solar convective zone are at least 10^{12}. As was pointed out by Thompson *et al.* (2003), understanding the dynamics of such a highly turbulent, complex structure must rely on numerical modeling. Unfortunately, computational capabilities are very limited, and only the past decade has given rise to a number of realistic three-dimensional (3D) modeling attempts (Miesch & Toomre 2009; Paternò 2010).

The majority of 3D numerical simulations of stellar differential rotation that have been

reported in the literature were performed using only a few different numerical codes. Two most widely used are the Anelastic Spherical Harmonic (ASH) code by Clune *et al.* (1999) and the Pencil code (`http://code.google.com/p/pencil-code/`) developed at Nordita, Nordic Institute for Theoretical Physics (Stockholm, Sweden). ASH is a spectral anelastic turbulent magneto-hydrodynamical (MHD) code, designed for spherical geometries. Its applications include MHD simulations of solar global convection summarized by Miesch (2005), tachocline studies by Brun & Zahn (2006), recent dynamo simulations by Brown *et al.* (2010), and more references therein. Pencil is a Direct Numerical Simulation (DNS) code designed for modeling weakly compressible turbulent flows and is applicable to general astrophysical plasmas. A recent insight into advances in the simulation of large-scale stellar dynamos was given by Brandenburg (2009). Another code, the finite-volume hydrodynamical code EULAG (Pruse *et al.* 2008), has recently been adopted for global simulations of solar convection by Ghizaru *et al.* (2010).

Present-day theoretical and numerical models seem to reproduce the observed characteristics of solar turbulent convection, but these are mean-field or LES models and are highly dependent on the model assumptions. On the other hand, the observational data are not precise enough to put more constraints on the models. An illustrative example is the thermal wind concept. A tiny temperature difference between the poles and the equator of the Sun may drive a differential rotation. For example, only a few degrees warmer poles may produce a solar-like differential rotation profile, but such a difference is not detectable by available probing techniques (Thompson *et al.* 2003). With the launch of the Helioseismic and Magnetic Imager (HMI) instrument onboard the Solar Dynamics Observatory (SDO) spacecraft, new high-quality observational data are expected which will produce valuable information about the global convection and differential rotation. We have adopted a fully compressible LES solver CharLES, recently developed at CTR, for this problem. With its capability to perform modeling on unstructured grids, CharLES offers a promising opportunity to resolve the thin tachocline and the subphotospheric shear layers together with the whole convective zone in a single simulation domain. Since the code is fully-compressible, it can deal with high specific-entropy gradients, and there is no need to induce artificial diffusivities, as in anelastic codes. The influence of different SGS models on the simulation results may be easily studied with this code.

2. Method

The CharLES solver employs a hybrid second-order central-difference, finite-volume method and a WENO scheme to discretize the Navier-Stokes and conserved scalar equations on unstructured grids (Ham 2008; Ham *et al.* 2010). For the cell interface flux, an HLLC Riemann solver is employed. A three-stage explicit Runge-Kutta scheme is used for time marching. The solver has been validated using a supersonic turbulent channel flow and a supersonic turbulent boundary layer flow. CharLES is implemented in C++, and it solves the governing equations on unstructured Finite-Volume grids. ParMetis (Karypis & Kumar 1998) is employed for domain decomposition to parallel processors. Communication between the processors is handled using MPI.

2.1. *Equations in rotating frame*

Consider a reference frame that is uniformly rotating with angular speed $\mathbf{\Omega}_0$. The velocity of the uniform rotation at $\mathbf{r}$ is $\mathbf{u}_0 = [\mathbf{\Omega}_0 \times \mathbf{r}]$. In this noninertial frame, terms need to be added to the energy and the momentum conservation laws from centrifugal and Coriolis forces. The resulting system of hydrodynamical equations is

$$\frac{\partial \rho}{\partial t} + \nabla \cdot (\rho \mathbf{u}) = 0, \tag{2.1}$$

$$\frac{\partial (\rho \mathbf{u})}{\partial t} + \nabla \cdot \left(\rho \mathbf{u}\mathbf{u} + p\hat{\mathrm{I}} \right) = \nabla \cdot \hat{\tau} + \rho \mathbf{g} - \rho \left(2 \left[\mathbf{\Omega}_0 \times \mathbf{u} \right] + \left[\mathbf{\Omega}_0 \times \left[\mathbf{\Omega}_0 \times \mathbf{r} \right] \right] \right), \tag{2.2}$$

$$\frac{\partial \left(\rho E \right)}{\partial t} + \nabla \cdot \left(\left(\rho E + p \right) \mathbf{u} \right) = \nabla \cdot \left(k \nabla T + \hat{\tau} \cdot \mathbf{u} \right) + \rho \mathbf{u} \cdot \mathbf{g} + Q_{rad}, \tag{2.3}$$

where

$$\rho E = \frac{p}{\gamma - 1} + \frac{\rho u^2}{2} - \frac{\rho u_0^2}{2} \tag{2.4}$$

is the total energy per unit volume, ρ and p are gas density and pressure, and $\mathbf{u}$ is velocity in the rotating frame. Symbol $\hat{\mathrm{I}}$ is a unit tensor, $\hat{\tau}$ is stress tensor, $\mathbf{g}$ is gravitational acceleration, k is the thermal conductivity coefficient, and Q_{rad} represents radiative source term. This system of equations is closed with an ideal gas law:

$$p = \rho R T / M, \tag{2.5}$$

where M is the molar mass.

For a Newtonian fluid, the stress tensor is given by

$$\tau_{ij} = \mu \left[\frac{\partial u_i}{\partial x_j} + \frac{\partial u_j}{\partial x_i} - \frac{2}{3} \delta_{ij} \left(\nabla \mathbf{u} \right) \right], \tag{2.6}$$

where $\mu = \rho \left(\nu_m + \nu_t \right)$ is the dynamic viscosity, ν_m is the molecular viscosity, and ν_t is the turbulent (eddy) viscosity, given by an implicit sub-grid scale (SGS) model. Since the molecular viscosity ν_m in solar plasma is negligibly small, we account for only the second term, for which we use the notation ν in what follows.

Similarly, the thermal conductivity $k = C_p \rho \left(\kappa_m + \kappa_t \right)$ can be split into two parts, associated with molecular diffusivity κ_m and eddy diffusivity κ_t. Throughout the convective zone of the Sun, heat conduction is negligibly small compared with convective transport, and κ_m may be ignored. Below we refer to the diffusivity simply as κ, and it comes entirely from the SGS model. The radiative source term Q_{rad} is also negligible compared with convective transport except in the uppermost part of the convective zone, $r > 0.98 R_\odot$ (Asplund *et al.* 2009), and we state $Q_{rad} = 0$ in our model.

2.2. *Model*

Our simulations are performed in a spherical shell that extends from the base of the convective zone $r_1 = 0.71 R_\odot$ to the upper convective zone $r_2 = 0.98 R_\odot$. The uniform rotation speed is set to the solar rotation rate observed at mid-latitudes: $\Omega_0 = 2.6 \times 10^{-6}$ rad/s. The initial unperturbed stratification of the thermodynamic parameters depends only on radius r and was taken from a standard solar model (Christensen-Dalsgaard *et al.* 1996). All computations are performed in Cartesian geometry, where the z axis coincides with the axis of solar rotation.

2.3. *Grid generation*

We perform grid generation via two approaches. The first method is to generate an unstructured hexahedral grid using FLUENT and GAMBIT. The second approach is to generate a structured grid with anisotropic refinement using the CTR in-house grid

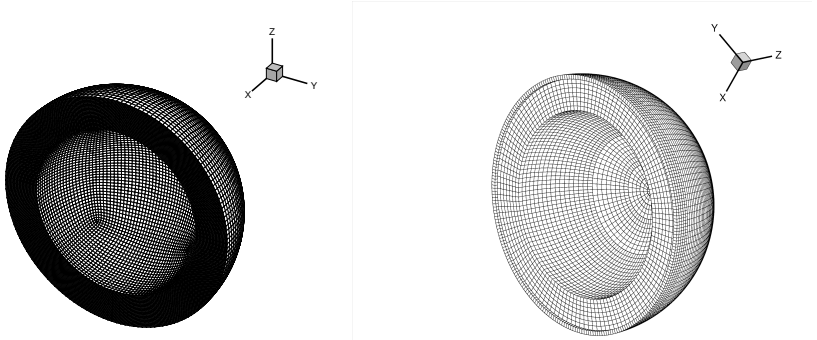

FIGURE 1. Left: hexahedral computational grid generated by FLUENT and GAMBIT. Right: computational grid generated by TOMMIE. Only half of the cells are shown in both cases.

TABLE 1. Parameters of the two runs

Parameter	Notation	Case 1	Case 2
Eddy viscosity (m^2/s)	ν	$1 \cdot 10^{11}$	$5 \cdot 10^{8}$
Prandtl number	$Pr = \nu/\kappa$	1.2	0.1
Rayleigh number[1]	Ra	$5.3 \cdot 10^{5}$	$1.7 \cdot 10^{9}$
Taylor number	Ta	3.4	$1.3 \cdot 10^{5}$
Rossby number[1]	Ro	20	200

[1]Estimated in the middle of the convective zone.

generator TOMMIE (Iaccarino & Ham 2007). Sample spherical shells generated by these two methods are presented in Figure 1.

2.4. *Boundary conditions*

We use stress-free isothermal conditions on the outer (top) boundary. On the inner (bottom) boundary, all velocity components are set to zero. This "sticks" the convective zone to the uniformly-rotating radiative core of the Sun and drives the rotation of the convective envelope. The inner boundary in our test runs is also isothermal. However, in realistic simulations, it is more physical to impose a constant energy flux through the bottom boundary to account for solar irradiance. Some aspects of boundary conditions in the simulations of global convection were discussed by Miesch *et al.* (2006).

3. Results

We present the results of two test simulations. They were performed on the unstructured grid with 1.5 million points (see Figure 1), at a maximum CFL number of 0.9. Both had the same initial background atmospheric stratification, but different viscosity ν and diffusivity κ. The parameters of the two runs are listed in Table 1.

The viscosity ν was kept constant throughout the model. Following Miesch *et al.* (2000),

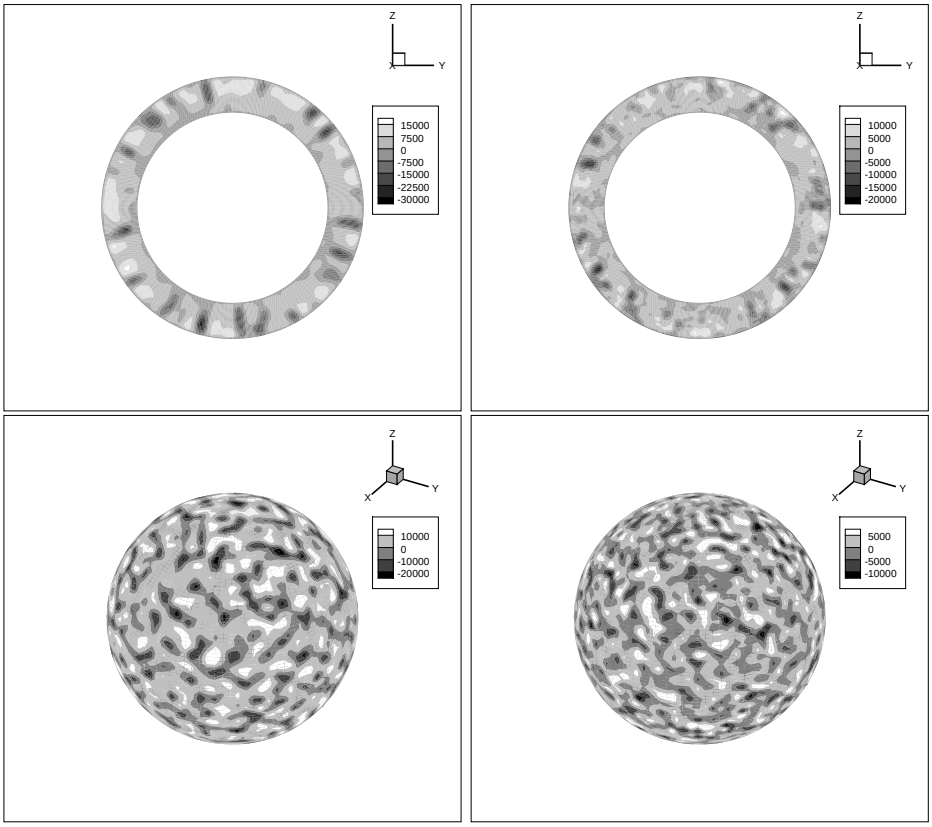

FIGURE 2. Top: radial velocity snapshots from the two simulations in the meridional plane. Bottom: radial velocity snapshots from the two simulations at $r = 0.92R_\odot$. The left panels correspond to the first, high-viscosity case, the right panels to the second case. The scale is given in m/s.

we set a constant Prandtl number Pr for all cells. The diffusivity was then computed as $\kappa = \nu/Pr$. In the first case, we have chosen a very high ν to make the system establish a stationary convection regime quickly. In the second case, the ν and Pr values were taken exactly the same as in the "Turbulent" simulation of Miesch *et al.* (2000). Note that the turbulent viscosity coefficient in our simulations could not be directly compared to the one from Miesch *et al.* (2000), where the viscous term in the energy equation is proportional to the specific entropy gradient. In the first case, a stationary mean energy distribution was established after 100 days of solar time, while in the second case, the mean kinetic energy density was still slowly growing, after 200 days of solar time.

We estimate the Rayleigh number as

$$Ra = \frac{gd^3}{\nu k}\frac{\Delta T}{T}, \tag{3.1}$$

where d is the shell thickness and ΔT is the temperature difference between the inner and outer boundaries. Although we haven't computed the critical Rayleigh number Ra_c, we expect $Ra_c \sim 10^3$, as in Miesch *et al.* (2000), because we used almost the same radial stratification of thermodynamical parameters. The ratio of Ra/Ra_c, or supercriticality, provides a measure of how high the convective instability is in the model. In both con-

sidered cases the supercriticality is much larger than 1, and convection is very efficient (Table 1).

The Taylor number, $Ta = 4\Omega^2 d^4/\nu^2$, characterizes the importance of the centrifugal force relative to viscous forces. In the first case $Ta \sim 1$ (Table 1), and viscous forces dominate the inertial ones. As was pointed out by Miesch *et al.* (2000), high Rayleigh and Taylor numbers are desirable to obtain a solar-like differential rotation profile. In the second case, the Taylor number is much higher.

Radial velocity v_r snapshots made for both cases after 100 days of solar time are shown in Figure 2. In the first case the surface area of the convective cells is large, and the cells span the entire convective zone. The downdrafts are concentrated in a narrower "lanes", surrounding the big rising convective cells. The downward velocities are almost twice as high as the upward velocities, and reach 30 km/s in the middle of the convective zone, which correspond to Mach numbers less than 0.2. In the second case the convection is much more turbulent, and the convective cells do not span through the thickness of the shell. The horizontal scale of downdrafts is smaller than the scale of upward-propagating cells. The downdrafts are also faster. The values of v_r in the second case are smaller than in the first one throughout the model. The convection pattern in the second case does not show the small-scale vortices obtained by Miesch *et al.* (2000). We assume this is due to a lack of spatial resolution in our test simulations. The connection between convection and rotation is estimated via a non-dimensional Rossby number: $Ro = \omega_{rms}/2\Omega$, where ω_{rms} is r.m.s. vorticity. If $Ro \sim 1$, the convective turnover time and rotation period are close, and convection is strongly affected by Coriolis forces. This is a necessary condition for differential rotation to be established. The estimated Rossby numbers in the middle of the convective zone in both simulations are $Ro \geq 20$ (Table 1), and convection is not coupled with rotation.

4. Future plans

The test simulations presented here have shown the capability of the CharLES numerical code to simulate turbulent convection in rotating spherical shells. The stationary convection process has been established in the first case, while in the second, low-viscosity case, the energy balance is still changing slowly. The tests presented here have pointed out the need for some improvements that should be made to the code and setup in order to obtain solar-like differential rotation. The turbulent vortices reported by others were not reproduced in our models, and the next necessary step is to increase grid resolution to be able to capture the vortices and to test the influence of various SGS models on the resulting convection pattern. In order to obtain Rossby numbers of order unity, and thereby to get strong coupling of rotation and convection, several runs should be made with various viscosity and Prandtl number values.

Once a qualitative agreement with existing models and observations of solar differential rotation have been obtained, the tachocline and the upper shear layer must be studied. For this, new grids with refinements in the necessary regions are required. Different regimes of differential rotation must be studied in order to reach the best agreement with observations. The magnetic induction equation and corresponding magnetic forces must be implemented in the code in order to study the solar dynamo.

Acknowledgments

Authors would like to thank Alan Wray for corrections made to this paper.

REFERENCES

Asplund, M., Nordlund, A. & Stein, R. F. 2009 Solar surface convection. *Living Reviews in Solar Physics* **6** (2).

Brandenburg, A. 2009 Advances in theory and simulations of large-scale dynamos. *Space Sci. Rev.* **144**, 87–104.

Brown, B. P., Browning, M. K., Brun, A. S., Miesch, M. S. & Toomre, J. 2010 Persistent magnetic wreaths in a rapidly rotating Sun. *Astrophys. J.* **711**, 424–438.

Brun, A. S. & Zahn, J. 2006 Magnetic confinement of the solar tachocline. *Astron. Astrophys.* **457**, 665–674.

Christensen-Dalsgaard, J. 2002 Helioseismology. *Reviews of Modern Physics* **74**, 1073–1129.

Christensen-Dalsgaard, J., Dappen, W., Ajukov, S. V., Anderson, E. R., Antia, H. M., Basu, S., Baturin, V. A., Berthomieu, G., Chaboyer, B., Chitre, S. M., Cox, A. N., Demarque, P., Donatowicz, J., Dziembowski, W. A., Gabriel, M., Gough, D. O., Guenther, D. B., Guzik, J. A., Harvey, J. W., Hill, F., Houdek, G., Iglesias, C. A., Kosovichev, A. G., Leibacher, J. W., Morel, P., Proffitt, C. R., Provost, J., Reiter, J., Rhodes, Jr., E. J., Rogers, F. J., Roxburgh, I. W., Thompson, M. J. & Ulrich, R. K. 1996 The current state of solar modeling. *Science* **272**, 1286–1292.

Clune, T. C., Elliott, J. R., Miesch, M. S., Toomre, J. & Glatzmaier, G. A. 1999 Computational aspects of a code to study rotating turbulent convection in spherical shells. *Parallel Comput.* **25**, 361–380.

Ghizaru, M., Charbonneau, P. & Smolarkiewicz, P. 2010 Magnetic cycles in global large-eddy simulations of solar convection. *Astrophys. J. Let.* **715**, L133–L137.

Gizon, L., Birch, A. C. & Spruit, H. C. 2010 Local helioseismology: three-dimensional imaging of the solar interior. *Annu. Rev. Astron. Astrophys.* **48**, 289–338.

Ham, F. 2008 Improved scalar transport for unstructured finite volume methods using simplex superposition. Center for Turbulence Research, Annual Research Brief.

Ham, F., Liang, C. & Terrapon, V. 2010 Hybrid central/WENO method for compressible large eddy simulation on unstructured grids. TFSA Conference 2010, Stanford University.

Iaccarino, G. & Ham, F. 2007 Les on cartesian grids with anisotropic refinement. *Lecture Notes in Computational Science and Engineering* **56**, 181–199.

Karypis, G. & Kumar, V. 1998 A parallel algorithm for multilevel graph partitioning and sparse matrix ordering. *J. Parallel Distrib. Comput.* **48**, 71–95.

Maeder, A. 2009 *Physics, Formation and Evolution of Rotating Stars*.

Miesch, M. S. 2005 Large-scale dynamics of the convection zone and tachocline. *Living Reviews in Solar Physics* **2**, 1–139.

Miesch, M. S., Brun, A. S. & Toomre, J. 2006 Solar differential rotation influenced by latitudinal entropy variations in the tachocline. *Astrophys. J.* **641**, 618–625.

Miesch, M. S., Elliott, J. R., Toomre, J., Clune, T. L., Glatzmaier, G. A. & Gilman, P. A. 2000 Three-dimensional spherical simulations of solar convection. I. Differential rotation and pattern evolution achieved with laminar and turbulent states. *Astrophys. J.* **532**, 593–615.

Miesch, M. S. & Toomre, J. 2009 Turbulence, magnetism, and shear in stellar interiors. *Annu. Rev. of Fluid Mechanics* **41**, 317–345.

Paternò, L. 2010 The solar differential rotation: a historical view. *Astrophys. Space. Sci.* **328**, 269–277.

Pruse, J. M., Smolarkiewicz, P. K. & Wyszogrodzki, A. A. 2008 Eulag, a computational model for multiscale flows. *Comput. Fluids* **37**, 1193–1207.

Schrijver, C. J. & Zwaan, C. 2000 *Solar and Stellar Magnetic Activity*.

Tassoul, J. 1978 *Theory of rotating stars*.

Thompson, M. J., Christensen-Dalsgaard, J., Miesch, M. S. & Toomre, J. 2003 The internal rotation of the sun. *Annu. Rev. Astron. Astrophys.* **41**, 599–643.